Synthesis, Characterization, and Properties of Microemulsion-Mediated Nanophase TiO_2 Particles

V. Chhabra, V. Pillai, B. K. Mishra, A. Morrone,† and D. O. Shah*

Center for Surface Science & Engineering, Department of Chemical Engineering, and Department of Materials Science & Engineering, University of Florida, Gainesville, Florida 32611

Received January 12, 1995. In Final Form: May 5, 1995®

Nanophase TiO_2 particles, with typical particle sizes in the range of 20–50 nm, have been synthesized using a microemulsion-mediated process. In this process, the aqueous cores of water/Triton X-100/hexanol/cyclohexane microemulsions have been used as constrained microreactors for the precipitation of precursor titanium hydroxide. The hydroxide particles thus formed were separated, dried, and calcined at different temperatures to form nanoparticles of TiO_2. In order to see the phase transition temperature, thermogravimetric analysis/differential thermal analysis studies were performed on the precursor hydroxide particles. The average particle size of these particles was determined by transmission electron microscopy, BET surface area and line broadening by X-ray diffraction. Phase transformation of these particles was confirmed by X-ray diffraction. The attenuation of ultraviolet radiation increased as the particle size decreased. As a catalyst for the photodegradation of phenol, only the anatase form of TiO_2 showed significant degradation of phenol, whereas the rutile form of TiO_2 was totally inactive for this reaction.

Introduction

Titania powders, widely used in industrial application as pigments, opacifiers, photocatalysts, and fillers, have been obtained either directly from titanium-bearing minerals or by precipitation from solutions of titanium salts. Titania exists in two tetragonal forms, a metastable phase, anatase, and a stable form, rutile. The volume free energy of the rutile phase is always lower than that of anatase. Therefore, on heat treatment, the anatase phase transforms to the stable rutile form. The transformation is a nonreversible metastable-to-stable transformation; the transition temperature reported in literature ranges from 450 to 1200 °C.[1] The transformation temperature depends on the nature and structure of the precursor and the preparation conditions. The majority of chemical methods of preparation yield the metastable anatase phase, which on further heat treatment gives the rutile phase. The most common procedure for the preparation of TiO_2 particles reported in literature is based on the hydrolysis of acidic solutions of Ti(IV) salts. In addition, gas-phase oxidation reactions of $TiCl_4$[2–4] and hydrolysis reactions of titanium alkoxides[5–7] have been employed to generate finely divided, high-purity TiO_2 powders. Jean *et al.*[7] have used hydroxypropyl cellulose to provide steric stabilization during the precipitation of TiO_2 particles to prevent agglomeration and synthesize monodispersed powders.

Nanophase ceramics with an average grain size of less than 100 nm have generated considerable scientific interest recently because of the improvements in a variety of properties that are expected to result from grain-size reduction to the nanometer scale. Many efforts has been directed toward the synthesis of submicron particles with a narrow size distribution for the preparation of nanophase ceramic materials[8–10] that have improved properties.[11,12] In most cases, the nanoparticles are synthesized in a vacuum or under low pressure by evaporation of a bulk source material. Titania particles have also been made by reaction in aerosols.[13,14] These nanophase materials have several technical applications like catalysis, lowering the sintering temperature, increasing the sintering rate, controlling the microstructure in high performance ceramic materials, and electronic and magnetic applications. The desirability of small and uniform particle size for obtaining quality ceramics has been documented in general[8] and for TiO_2 specifically.[15,16] In this respect, we have made an attempt to produce monodispersed, high-purity TiO_2 particles using monodispersed aqueous droplets of water-in-oil microemulsions as microreactors. We have characterized the TiO_2 nanoparticles synthesized using microemulsions and studied the attenuation of ultraviolet radiation as a function of the size of the TiO_2 particles. We have also used these particles as photocatalysts to study the photodegradation of phenol, which is a common contaminant in many waste water streams.

Microemulsions as Microreactors

A microemulsion may be defined as a thermodynamically stable, optically isotropic solution of two immiscible liquids (e.g. water and oil) consisting of microdomains of one or both liquids stabilized by an interfacial film of

† Department of Materials Science & Engineering.

® Abstract published in *Advance ACS Abstracts,* July 15, 1995.

(1) Kumar, P. N. K. Ph.D Thesis, University of Twente, 7500 AE Enschede, The Netherlands, 1993.
(2) Formenti, M.; Juillet, F.; Meriiaudeau, P.; Teichner, S. J.; Vergnon, P. *J. Colloid Interface Sci.* **1972**, *39*, 79.
(3) George, A. P.; Murley, R. D.; Place, E. R. *Faraday Symp. Chem. Soc.* **1973**, *7*, 63.
(4) Suyama, Y.; Kato, A. J. *Am. Ceram. Soc.* **1976**, *56*, 146.
(5) Mazdiyasni, K. S. *Ceram. Int.* **1982**, *8*, 42.
(6) Yan, M.; Rhodes, W.; Springer, L. *Am. Ceram. Soc. Bull.* **1982**, *61*, 911.
(7) Jean, J. H.; Ring, T. A. *Colloids Surf.* **1988**, *29*, 273.
(8) Bowen, H. K. *Mater. Sci Eng.* **1980**, *44*, 1 and references therein.
(9) Matijevic, E. *Mater. Res. Soc. Bull.* **1989**, *14*, 18 and references therein.
(10) Matijevic, E. *Mater. Res. Soc. Bull.* **1990**, *15*, 16 and references therein.
(11) Siegel, R. W.; Ramasamy, S.; Hahn, H.; Zongquan, L.; Ting, L.; Gronsky, R. *J. Mater. Res.* **1988**, *3*, 1367.
(12) Hahn, H.; Logas, J.; Averback, R. S. *J. Mater. Res.* **1990**, *5*, 609.
(13) Morooka, S.; Kusakabe, K. *Powder Sci Tech.* **1988**, *6*, 65.
(14) Salmon, R.; Matijevic, E. *Ceram. Int.* **1990**, *16*, 157.
(15) Barringer, E. A.; Bowen, H. K. *J. Am. Ceram. Soc.* **1982**, *65*, C-199.
(16) Fegley, B. Jr.; Barringer, E. A.; Bowen, H. K. *J. Am. Ceram. Soc.* **1984**, *67*, C-113.

0743-7463/95/2411-3307$09.00/0

Table 1. Composition of Microemulsion Systems Used for Synthesis Reaction

	microemulsion I	microemulsion II	wt fraction
aqueous phase	$TiCl_4$ solution (0.3 M)	ammonia solution (1.2 M)	0.08
surfactant	Triton X-100	Triton X-100	0.19
cosurfactant	*n*-hexanol	*n*-hexanol	0.15
oil phase	cyclohexane	cyclohexane	0.58

surfactant.[17,18] The surfactant molecule generally has a polar (hydrophilic) head group and a long-chained aliphatic (hydrophobic) tail. Such molecules optimize their interactions by residing at the oil/water interface, thereby considerably reducing the interfacial tension. In water-in-oil microemulsions, the aqueous phase is dispersed as microdroplets (typically 10−25 nm in size) surrounded by a monolayer of surfactant molecules in the continuous hydrocarbon phase. The aqueous cores of microemulsions, containing soluble metal salts, are used as microreactors for the synthesis of nanoparticles. Due to the dynamic nature of the microdroplets, the exchange mechanism involves coalescence and fusion of the droplets upon collision, which then disintegrate into droplets, and this process occurs continuously in the microemulsion.[19] If two reactants, A and B, are dissolved in the aqueous core of two identical water-in-oil microemulsions, upon mixing they will form a precipitate, AB. The growth of these particles in microemulsions is suggested to involve interdroplet exchange and nuclei aggregation.[20,21]

Microemulsions were first used by Boutonnet *et al.*[22] to obtain ultrafine monodispersed metal particles of Pt, Pd, Rh, and Ir by reducing corresponding salts in the aqueous droplets of water-in-oil microemulsions with hydrazine or hydrogen gas. Kurihara *et al.*[23] have carried out studies on laser and pulse radiolytically induced colloidal gold formation in water-in-oil microemulsions. Henglein and co-workers[24,25] have used similar techniques for the production of nanometer-sized metal and semiconductor particles by radiolytic reduction. Water-in-oil microemulsions have also been used to synthesize nanoparticles of metal borides,[26] silver halides,[27,28] $BaCO_3$,[29] the oxalate precursor for $YBa_2Cu_3O_{7-x}$ superconductor,[30] and barium–iron carbonate[31] for preparation of barium ferrite particles. Recently, ultrafine TiO_2 particles have been generated in water-in-oil microemulsions by Joselevich *et al.*[32] and Arriagada *et al.*[33] In this paper, we report the synthesis of TiO_2 nanoparticles using water-in-oil microemulsions composed of TX-100, cyclohexane, and hexanol and studies on the effect of the calcination temperature on the phase and particle size of TiO_2 particles and on technological applications of TiO_2 particles with respect to the effect of particle size on attenuation of ultraviolet radiation and photocatalyst.

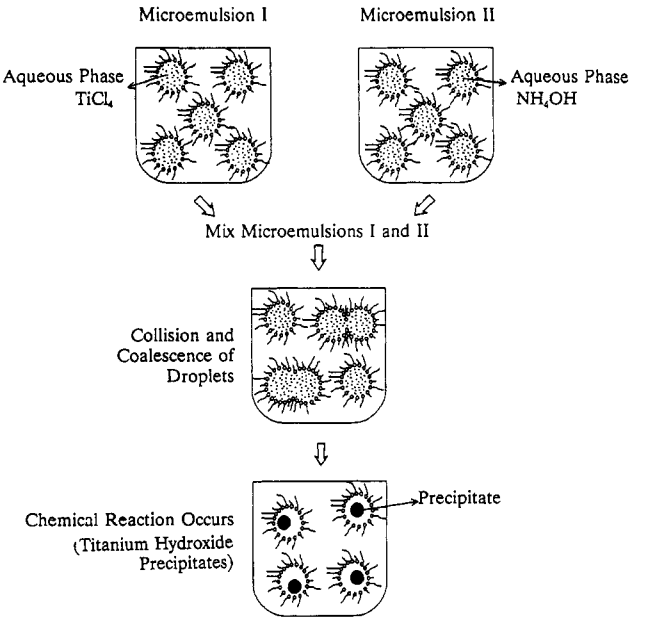

Figure 1. Schematic diagram showing the preparation of TiO_2 particles in microemulsions.

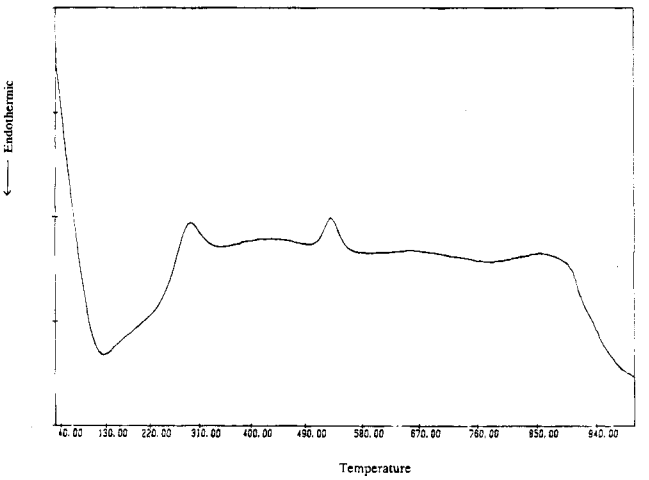

Figure 2. Differential thermal analysis of the hydroxide precursor in the presence of air (20 cm^3/min), weight = 5 mg, scan rate = 10 °C/min.

Experimental Procedure

Materials. Titanium tetrachloride was purchased from Sigma. Ammonia solution, Triton X-100, *n*-hexanol, cyclohexane, and phenol (crystals) were purchased from Aldrich Chemical Co. Methanol and chloroform were purchased from Fisher. All reagents were used without further purification. Water was deionized and distilled before use.

Methods. We selected a microemulsion with Triton X-100 as the surfactant, *n*-hexanol as co-surfactant, cyclohexane as the continuous oil phase, and electrolyte solution as the dispersed aqueous phase.

(17) De Gennes, P. G.; Taupin, C. *J. Phys. Chem.* **1982**, *86*, 2294.
(18) Leung, R.; Hou, M. J.; Manohar, C.; Shah, D. O.; Chun, P. W. In *Macro- and Microemulsions;* Shah, D. O., Ed.; American Chemical Society: Washington DC, 1981; p 325.
(19) Eicke, H. F.; Shepherd, J. C. W.; Steinemann, A. *J. Colloid Interface Sci.* **1976**, *56*, 168.
(20) Fendler, J. H. *Chem. Rev.* **1987**, *87*, 877.
(21) Sugimoto, T. *Adv. Colloid Inter. Sci.* **1987**, *28*, 65.
(22) Boutonnet, M.; Kizling, J.; Stenius, P.; Maire, G. *Colloids Surf.* **1982**, *5*, 209.
(23) Kurihara, K.; Kizling, J.; Stenius, P.; Fendler, J. H. *J. Am. Chem. Soc.* **1983**, *105*, 2574.
(24) Haase, M.; Weller, H.; Henglein, A. *Ber. Bunsenges. Phys. Chem.* **1988**, *92*, 1103.
(25) Kumar, A.; Henglein, A.; Weller, H. *J. Phys. Chem.* **1989**, *93*, 2262.
(26) Lumfimpadio, N.; Nagy, J. B.; Derouane, E. G. In *Surfactants in Solution*; Mittal, K. L., Lindman, B., Eds.; Plenum: New York, 1986; Vol. 3, p 483.
(27) Hou, M. J.; Shah, D. O. In *Interfacial Phenomena in Biotechnology and Material Processing;* Attia, Y. A., Moudgil, B. M., Chander. S., Eds.; Elsevier: Amsterdam, 1988; p 443.
(28) Chew, C. H.; Gan, L. M; Shah, D. O. *J. Dispersion Sci. Technol.* **1990**, 11, 593.
(29) Kon-no, K.; Koide, M.; Kitahara, A. *J. Chem. Soc. Jpn.* **1984**, *6*, 815.
(30) Ayyub, P.; Maitra, A. N.; Shah, D. O. *Physica C* **1990**, *168*, 571.
(31) Pillai, V.; Kumar, P.; Shah, D. O. *J. Magn. Mag. Mater.* **1992**, *116*, L-299.
(32) Joselvich, E.; Willner, I. *J. Phys. Chem.* **1994**, *98*, 7628.
(33) Arriagada, F. J.; Osseoassare, K. *J. Dispersion Sci. Technol.* **1994**, *15*, 59.

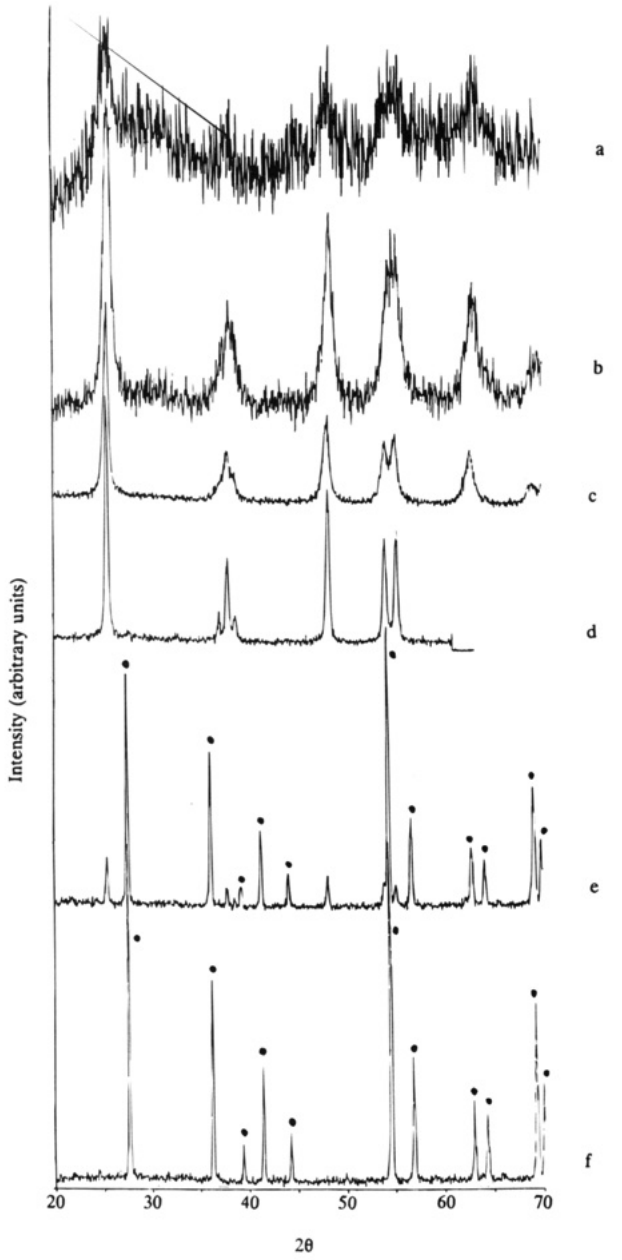

Figure 3. X-ray diffractograms of the samples calcined at (a) 400 °C, (b) 600 °C, (c) 700 °C, (d) 800 °C, (e) 900 °C, and (f) 1000°C. All peaks marked with ● are for the rutile phase and rest of them are for the anatase phase.

Microemulsions were prepared by solubilizing different electrolytes into Triton X-100/*n*-hexanol/cyclohexane solutions. We took two microemulsions (microemulsion I and microemulsion II) with identical composition (Table 1) but a different aqueous phase. The aqueous phase in microemulsion I was an aqueous solution (0.3 M) of $TiCl_4$, whereas the aqueous phase in microemulsion II was the precipitating agent ammonium hydroxide (1.2 M). These two microemulsions were mixed with vigorous stirring at room temperature. Due to the continuous collisions and coalescence of the droplets of water-in-oil microemulsions,[19] the reacting species in microemulsions I and II ($TiCl_4$ and ammonium hydroxide, respectively) come in contact with each other and react. This leads to the precipitation of titanium hydroxide within the aqueous cores of the microemulsion. A schematic diagram for the preparation of TiO_2 particles in microemulsion is shown in Figure 1. The particles thus prepared in the constrained microreactors of microemulsion droplets are expected to be fairly uniform and homogeneous and have a higher surface area with very small particle size.

The precipitate was separated in a Sorvall RC-5B Superspeed centrifuge at 10 000 rpm for about 10 min. The precipitate was then thoroughly washed in a 1:1 mixture of methanol and chloroform followed by pure methanol to remove the contaminated oil and surfactant from the particles. The precipitate was then dried at 100 °C.

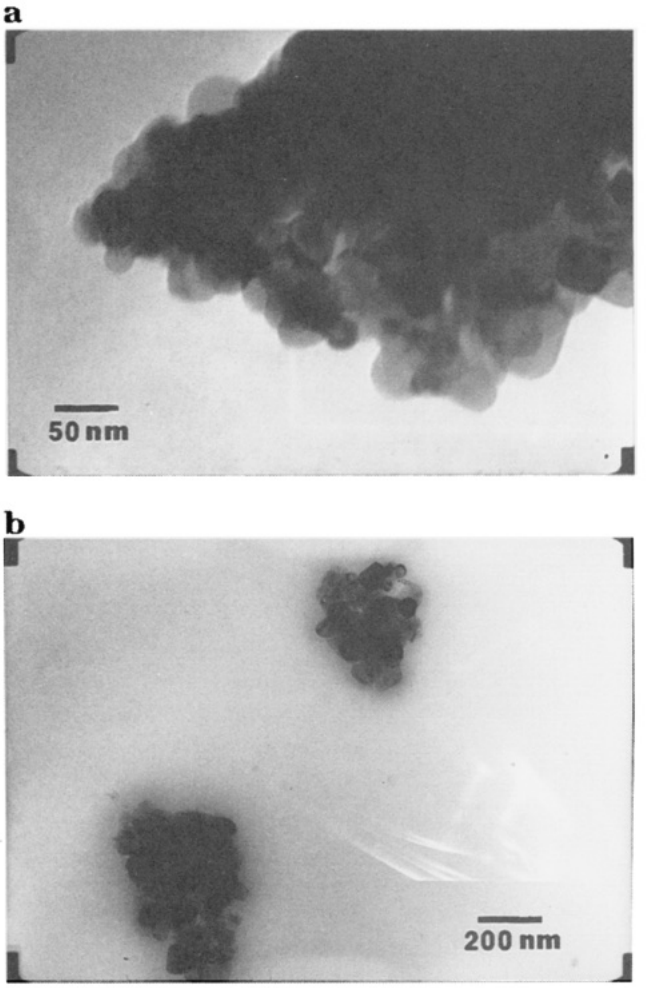

Figure 4. Transmission electron micrographs for samples calcined at (a) 700 °C and (b) 1000 °C.

Thermogravimetric analysis (TGA) of the precursor was recorded on a TGA/DTA instrument in air with a heating rate of 10 °C/min. Differential thermal analysis (DTA) was done on the dried powder in air with a heating rate of 10 °C/min.

Transmission electron microscopy (TEM) was used to study the size and size distribution of the calcined particles. TEM of these samples was done by ultrasonically dispersing the powders in methanol prior to deposition on a carbon-coated TEM grid. A JEOL 200 CX transmission electron microscope was used for these studies. For better analysis, a large number of photographs were examined.

Phase analysis of the calcined powders was carried out by a powder X-ray diffraction (XRD) method using a Phillips PW 1700 powder diffractometer, which works on the Bragg–Bentano principle. All the measurements were done at room temperature using Cu Kα radiation ($\lambda = 1.5405$ Å) at 40 kV and 20 mA. The specimen was mounted in the center of the diffractometer and rotated by an angle (θ) around an axis in the plane.

The total surface area of the particles was measured using a Quantasorb BET surface area analyzer by Quantachrome Corp. Previously adsorbed gases were removed prior to the measurement by degassing the samples in nitrogen gas at 110 °C for 20 h. A known mixture of nitrogen (adsorbent) and helium (carrier) gas was passed through the sample cell. When the sample cell is immersed in liquid nitrogen, the sample adsorbs nitrogen. The amount of nitrogen adsorbed was measured for three different nitrogen/helium ratios, and the surface area was calculated using the BET equation.

A photoreactor fitted with a lamp was used to perform the photocatalytic experiments. The volume of the reactor was 250

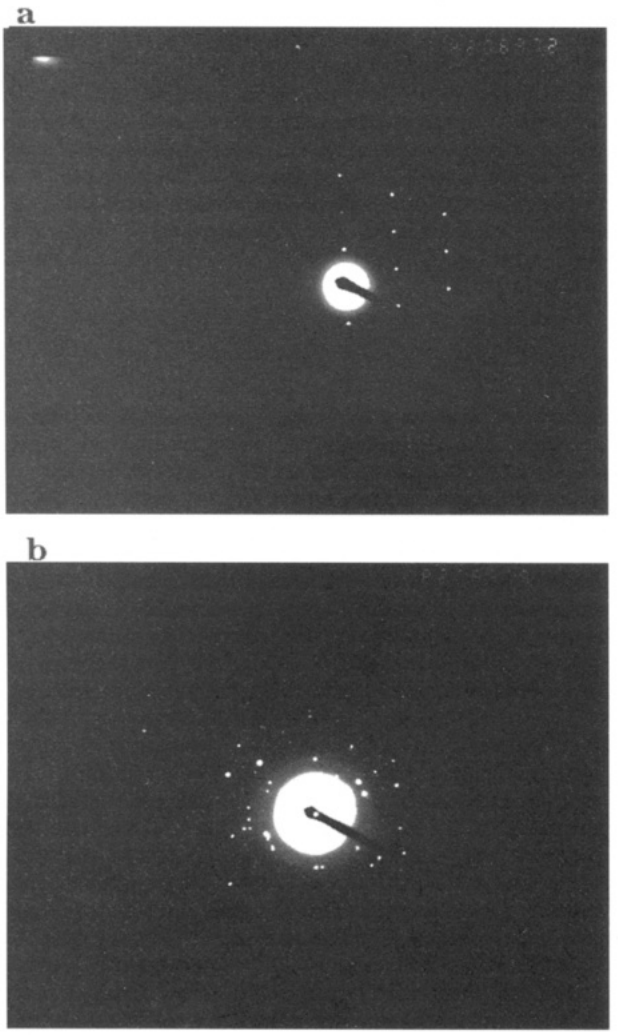

Figure 5. Electron diffraction photograph for samples calcined at (a) 700 °C and (b) 1000 °C.

mL, and continuous stirring was used to maintain both concentration and uniform temperature. A 300 W medium pressure lamp was used as the light source. A measured quantity of catalyst powder (1 g/L of phenol solution 0.02% w/v in water) was always used to study the photodegradation of phenol. The photodegradation runs lasted several hours and samples were withdrawn for analysis every hour. The samples were immediately centrifuged and the phenol concentration in the supernatant liquid was measured spectrophotometrically.

Optimization of particle size for ultraviolet absorption has been done by measuring the transmittance of solution with suspended TiO_2 particles. The TiO_2 suspension was made in a 1:1 (v/v) mixture of water and polyethylene glycol. These samples were ultrasonically dispersed before measuring the transmittance.

Results and Discussion

The structural aspects of TiO_2 particles were studied by a number of techniques such as TGA/DTA, XRD, TEM, and BET surface area. For thermal analysis, the precursor sample (about 0.5 g) was heated in a stream of air, having a flow rate of 20 cm^3/min, at a heating rate of 10 °C/min. The thermogravimetric studies showed that loss of mass began at 130 °C and was complete at 470 °C; no further change in weight took place upon continuing the heating up to 1000 °C. The DTA data (Figure 2) showed an endothermic dehydration peak at 130 °C and three exothermic peaks at 300, 530, and 890 °C, respectively. The first exotherm corresponds to dehydroxylation and removal of residual organics, while the other two appear to be due to structural transformations. This is also suggested by the fact that there is no further weight loss taking place corresponding to two exotherms at 530 and 890 °C. Of the two exotherms which are due to structural transformations, the first one represents the transformation of amorphous material to metastable anatase phase, and the second isotherm represents the conversion of the metastable anatase phase to the stable rutile phase. Hence, the following sequence of transitions occurs on heating of the sample:

$$TiO_2\ (\text{amorphous}) \xrightarrow{530\ ^\circ C} TiO_2\ (\text{anatase}) \xrightarrow{890\ ^\circ C} TiO_2\ (\text{rutile})$$

For the decomposition of the precursor, the samples were calcined at different temperatures, 200, 400, 600, 800, 1000 °C, for 2 h in air. Powder XRD was used for (i) identification of phases present and (ii) calculation of the average particle size using Scherrer's equation under the assumption that the powder sample consisted of small cubic crystals and the size distribution of the particles is the sole cause of line broadening. However, it is not a bad approximation to apply Scherrer's equation to the peak breadths of noncubic materials.[34] Figure 3 shows the XRD pattern of the calcined product at different temperatures. Powder XRD data of the samples calcined at 400 °C indicate that they are amorphous. The sample calcined at 600 °C is not completely crystalline but is dominated by the anatase phase. The diffractogram of the sample calcined at 800 °C was found to contain all the peaks characteristic of the anatase phase, and the 1000 °C sample was found to be pure rutile phase. In order to identify the proximity of the phase transition temperature, we also calcined the material at 700 and 900 °C. Powder XRD data show that the sample that calcined at 700 °C was anatase and the 900 °C sample was a mixture of both the anatase and rutile phases. The particle sizes calculated for these particles from Scherrer's equation are found to be in reasonable agreement with those observed in the transmission electron micrograph (TEM).

TEMs for the samples calcined at 700 (anatase) and 1000 °C (rutile) are shown in parts a and b of Figure 4, respectively. These micrographs show agglomerates of nanoparticles. The individual particles have a size range of 15−30 nm for the anatase phase and 40−60 nm for the rutile phase. This is in reasonable agreement with the average particle size calculated from the line broadening of the XRD (26 and 53 nm). In addition, electron diffraction photographs were also obtained for these samples (Figure 5). The pictures showed moderately sharp rings which match with the 'd' spacing for anatase and rutile.

Photocatalysis is one of a number of advanced oxidation technologies under consideration for the treatment of contaminated water.[35] Photocatalysis has received much attention as a possible tool for photochemical conversion and storage of energy. While this goal has not been reached as yet, photocatalytic processes are rapidly developing in the field of pollutants. Pollutants such as polychlorinated biphenyls, aromatic hydrocarbons, chlorinated alkanes, chloromethanes, oxalic acid, and chlorinated aromatic compounds have been photocatalytically degraded using various semiconductors, especially TiO_2.[36−43] Phenol has been chosen for the reaction because

(34) Warren, B. E. *X-Ray Diffraction*; Dover Publications, Inc.: New York, 1990; Chapter 13.

(35) Braun, A. M. In *Progress in the Applications of Photochemical Conversion and Storage*; Pelizzetti, E., Schiavello, Eds.; Kluwer Academic Publishers: Dordrecht, 1991; p 551.

(36) Augliaro, V.; Palmisano, L.; Sclafani, A.; Minero, C.; Pleizetti, E. *Toxicol. Environ. Chem.* **1988**, *16*, 89.

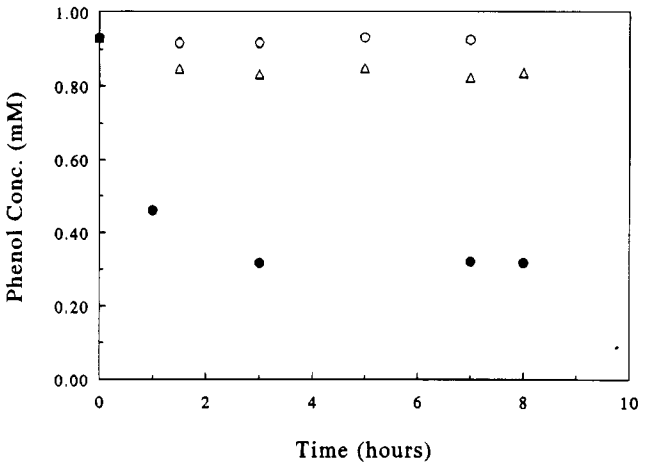

Figure 6. Photodegradation of phenol (1 g/L of phenol solution, 0.02% w/v in water) in presence of, (○) rutile TiO_2 particles and (●) anatase TiO_2 particles and (△) without catalyst.

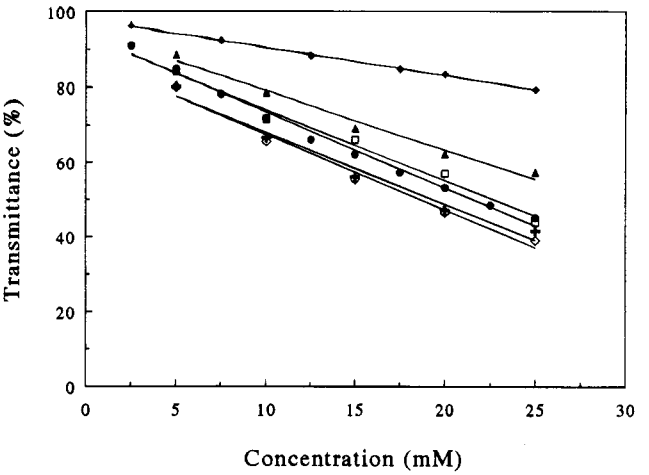

Figure 7. UV transmittance measurements of solutions with suspended TiO_2 particles calcined at different temperatures: (◇) precursor, (+) 200 °C, (□) 400 °C, (●) 600 °C, (▲) 800 °C, (◆) 1000 °C.

it is one of the most common contaminants in waste water streams.[44,45] Figure 6 shows the photodegradation of phenol in a photoreactor having a 300 W medium pressure lamp. The disappearance of phenol was analyzed spectrophotometrically. A blank test was also performed in the same reactor with the same lamp. It has been observed that only the anatase form is active for the photodegradation of phenol and the rutile form is totally inactive for this reaction. Auguliaro *et al.*[37] have systematically studied the photodegradation of phenol and given a mechanistic and kinetic model which accounts for their results and they have also given some likely reasons for the inactivity of rutile for this reaction.

In order to find the optimum size for the attenuation of ultraviolet radiation, we have made an attempt to measure the transmittance of a TiO_2 suspension in a 1:1 mixture of water and polyethylene glycol. Figure 7 shows the UV transmittance of TiO_2 particles calcined at different temperatures. It is clear from the graph that the particles calcined at lower temperature absorb more ultraviolet radiation and the amount of absorption decreases with an increase in calcination temperature. To see the effect of particle size on the attenuation of UV radiation, we measured the surface area of these particles using BET surface area (Table 2). It has been found that surface area decreases with an increase in calcination temperature. So it is clear from these results that the amount of UV absorption increases with a decrease in the size of the TiO_2 particles.

Table 2. BET Surface Area of TiO_2 Particles Calcined at Different Temperatures

calcination temperature (°C)	surface area (m^2/g)	calcination temperature (°C)	surface area (m^2/g)
0 (precursor)	333.01	700	42.82
200	301.34	800	12.01
400	134.79	900	6.23
600	57.07		

Conclusions

In this paper, we have presented a microemulsion-mediated process for the synthesis of ultrafine nanoparticles of TiO_2. Aqueous microdroplets of water-in-oil microemulsions have been used as microreactors to precipitate the precursor hydroxide of titanium(IV). These precursor particles have been calcined at different temperatures to produce ultrafine TiO_2 particles, as confirmed by X-ray diffraction. We have thus determined the calcination temperature required for complete transformation of the anatase phase to the rutile one. We also see that as calcination temperature is decreased, the surface area of the particles decreases, and therefore, the particle size increases. This is in agreement with the TEM micrographs. Furthermore, we have shown that the attenuation of ultraviolet radiation increases as the size of the TiO_2 particles decreases. We have also shown that only the anatase TiO_2 particles act as photocatalyst for photodegradation of phenol and the rutile form is totally inactive for this reaction.

Acknowledgment. The authors thank the National Science Foundation (Grant CTS 8922574), NSF-Engineering Research Center (Grant 9402989), and Alcoa Foundation for providing financial support for this research.

LA950022C

(37) Carey, J. H.; Lawrence, J.; Tosine, H. M. *Bull. Environ. Contam. Toxicol.* **1976**, *16*, 697.
(38) Child, L. P.; Ollis, D. F. *J. Catal.* **1980**, *66*, 383.
(39) Gab, S.; Schmitzer, J.; Tamm, H. W.; Parlar, H.; Korte, F. *Nature* **1977**, *270*, 331.
(40) Pruden, A. L.; Ollis, D. F. *J. Catal.* **1983**, *82*, 404.
(41) Hsiao, C. Y.; Lee, C. L.; Ollis, D. F. *J. Catal.* **1983**, *82*, 418.
(42) Barbeni, M.; Pramauro, E.; Pelizzetti, E.; Borgarello, E.; Serpone, N. *Chemosphere.* **1985**, *14*, 195.
(43) Matthews, R. W.; McEvoy, S. R. *Solar Energy* **1992**, *49*, 507.
(44) Sclafani, A.; Davi, E.; Palmisano, L.; Schiavello, M.; Sclafani, A. *J. Photochem. Photobiol. A: Chem.* **1991**, *56*, 113.
(45) Matthews, R. W.; McEvoy, S. R. *J. Photochem. Photobiol. A: Chem.* **1988**, *64*, 231.